Article

Not peer-reviewed version

Synthesis and Characterization of New Derivatives of (EZ)-N'-Benzylidene-(2RS)-2-(6-Chloro-9H-Carbazol-2-Yl)propanohydrazide as Potential Tuberculostatic Agents

Ilinca Margareta Vlad , Diana Camelia Nuță * , Miron Theodor Căproiu , Florea Dumitrașcu , Eleonóra Kapronczai , Georgiana Ramona Mük , Speranta Avram , Adelina Gabriela Niculescu , Irina Zarafu , Vanesa Alexandra Ciorobescu , Ana Maria Brezeanu , Carmen Limban

Posted Date: 19 January 2024

doi: 10.20944/preprints202401.1456.v1

Keywords: N-acyl hydrazone derivatives; microwave synthesis; FT-IR spectral data; NMR analysis; HRMS analysis; tuberculostatic activity.

Article

Synthesis and Characterization of New Derivatives of (*EZ*)-N'-Benzylidene-(2*RS*)-2-(6-chloro-9*H*-carbazol-2-yl)propanohydrazide as Potential Tuberculostatic Agents

Ilinca Margareta Vlad [1], Diana Camelia Nuță [1,*], Miron Theodor Căproiu [2], Florea Dumitrașcu [2], Eleonora Kapronczai [3], Georgiana Ramona Mük [4,5], Speranta Avram [4], Adelina Gabriela Niculescu [6,7], Irina Zarafu [8], Vanesa Alexandra Ciorobescu [1], Ana Maria Brezeanu [1] and Carmen Limban [1]

[1] Department of Pharmaceutical Chemistry, Faculty of Pharmacy, "Carol Davila" University of Medicine and Pharmacy, Traian Vuia no.6, 020956 Bucharest, Romania; ilinca.vlad@umfcd.ro; diana.nuta@umfcd.ro; ana.brezeanu@stud.umfcd.ro; vanesa-alexandra.buzatu@rez.umfcd.ro; carmen.limban@umfcd.ro

[2] "C. D. Nenitzescu" Institute of Organic and Supramolecular Chemistry, 202B Splaiul Independenței, 060023, Bucharest, Romania; fdumitra@yahoo.com; dorucaproiu@gmail.com

[3] Department of Chemistry, Supramolecular Organic and Organometallic Chemistry Centre, Faculty of Chemistry and Chemical Engineering, Babeş-Bolyai University, 11 Arany János, 400028 Cluj-Napoca, Romania; erzsebet.denes@ubbcluj.ro

[4] Faculty of Biology, University of Bucharest, Splaiul Independenței 91-95, Bucharest, R-050095, România; mukramonageorgiana@yahoo.com, speranta.avram@bio.unibuc.ro

[5] "St. Stephen's" Pneumoftiziology Hospital, Șoseaua Ștefan cel Mare 11, Bucharest, 020122, România

[6] Research Institute of the University of Bucharest, Sos. Panduri 90-92, Bucharest, R-050095, România; adelina.niculescu@upb.ro

[7] Department of Science and Engineering of Oxide Materials and Nanomaterials, National University of Science and Technology Politehnica Bucharest, 011061 Bucharest, Romania

[8] Department of Organic Chemistry, Biochemistry and Catalysis, Faculty of Chemistry, University of Bucharest, 4-12 Regina Elisabeta, 030018 Bucharest, Romania.zarafuirina@yahoo.fr

* Correspondence: diana.nuta@umfcd.ro

Abstract: N-acyl hydrazone (NAH) is recognized as a promising framework in drug design due to its versatility, straightforward synthesis, and attractive range of biological activities, including antimicrobial, antitumoral, analgesic, and anti-inflammatory properties. In the global context of increasing resistance of pathogenic bacteria to antibiotics, NAHs represent potential solutions for developing improved treatment alternatives. Therefore, this research introduces six novel derivatives of (*EZ*)-N'-benzylidene-(2*RS*)-2-(6-chloro-9*H*-carbazol-2-yl)propanohydrazide, synthesized using a microwave-assisted method. In more detail, we have joined two pharmacophore fragments in a single molecule, represented by an NSAID-type carprofen structure and a hydrazone-type structure, obtaining a new series of NSAID-N-acyl hydrazone derivatives that were further characterized spectrally using FT-IR, NMR, and HRMS investigations. Additionally, the substances were assessed for their tuberculostatic activity by examining their impact on four strains of *M. tuberculosis*, including two susceptible to rifampicin (RIF) and isoniazid (INH), one susceptible to RIF and resistant to INH and one resistant to both RIF and INH). The results of our research highlight the potential of the prepared compounds in fighting against antibiotic-resistant *M. tuberculosis* strains.

Keywords: N-acyl hydrazone derivatives; microwave synthesis; FT-IR spectral data; NMR analysis; HRMS analysis; tuberculostatic activity

1. Introduction

The principal pharmacophore scaffold, N-acyl hydrazone (NAH), consists of both amide and imine functional groups, potentially displaying geometrical and conformational stereoisomerism [1].

Preprints (www.preprints.org) | NOT PEER-REVIEWED | Posted: 19 January 2024 doi:10.20944/preprints202401.1456.v1

Rotation along the imine bond can generate two geometrical stereoisomers, the *E* and *Z* forms, while rotation across the amide bond can lead to conformational stereoisomerism, NAH being able to exist as *syn*periplanar and *anti*periplanar conformers [2].

NAHs have demonstrated remarkable versatility, showing promising outcomes in both drug design and drug chemistry. This adaptability is attributed to the straightforward synthesis of NAHs. Typically, these compounds are created by combining aldehydes or ketones with hydrazides. Notably, their distinctive structural characteristics encompass the presence of two geometric isomers, *E* and *Z*, in relation to the C=N bond plane. Additionally, there are two conformers arising from the rotation around the C-N bond within the amidic group.

The N-acyl hydrazone fragment has been identified in a large number of compounds acting on different targets [3-8]. NAHs are recognized for their antibacterial [9-12], antimycobacterial [13-15], antiprotozoal [16-20], antiviral [21], antitumoral [22], analgesic and anti-inflammatory properties [23]. Moreover, NAHs are important chemical intermediates for obtaining heterocyclic structures and ligands for forming metallic complexes [24]. Certain derivatives serve as fluorescent and colorimetric chemosensors employed in the detection of metals and anions [25].

There exist medicinal substances based on NAH (Figure 1), counting nitrofurazone (broad spectrum topical antibacterial agent) [26], nitrofurantoin (oral antibacterial agent for treating gastrointestinal tract infections) [27], nifuroxazide (antibacterial agent of use in gastrointestinal infections), carbazochrome (hemostatic agent, tested with good results against hereditary hemorrhagic telangiectasia) [28,29], dantrolene and azumolene (approved for the treatment of malign hyperthermia) [30,31], aldoxorubicin (a hydrazone derivative of doxorubicin, specifically a maleinimidoalkanoyl hydrazone), which functions as an albumin-binding prodrug of doxorubicin that reached phase III clinical trials for treating metastatic soft tissue sarcoma with deep localization; it releases doxorubicin at the target site with less systemic adverse effects, including lack of cardiotoxicity [32], LASSBio-294 ((2-thienylidene)-3,4-methylenedioxybenzoylhydrazine) (under preclinical testing for the treatment of heart failure) [33,34], and PAC-1 ((4-benzylpiperazino)acetic acid-(3-allyl-2-hydroxybenzylidene)hydrazide) (procaspase activator that reached clinical studies testing stage in 2015). In terms of the correlation between structure and activity, the segment of PAC-1, denoted by ortho-hydroxy-N-acyl hydrazone, plays a crucial role in binding Zinc and triggering the activation of procaspase 3 [35,36].

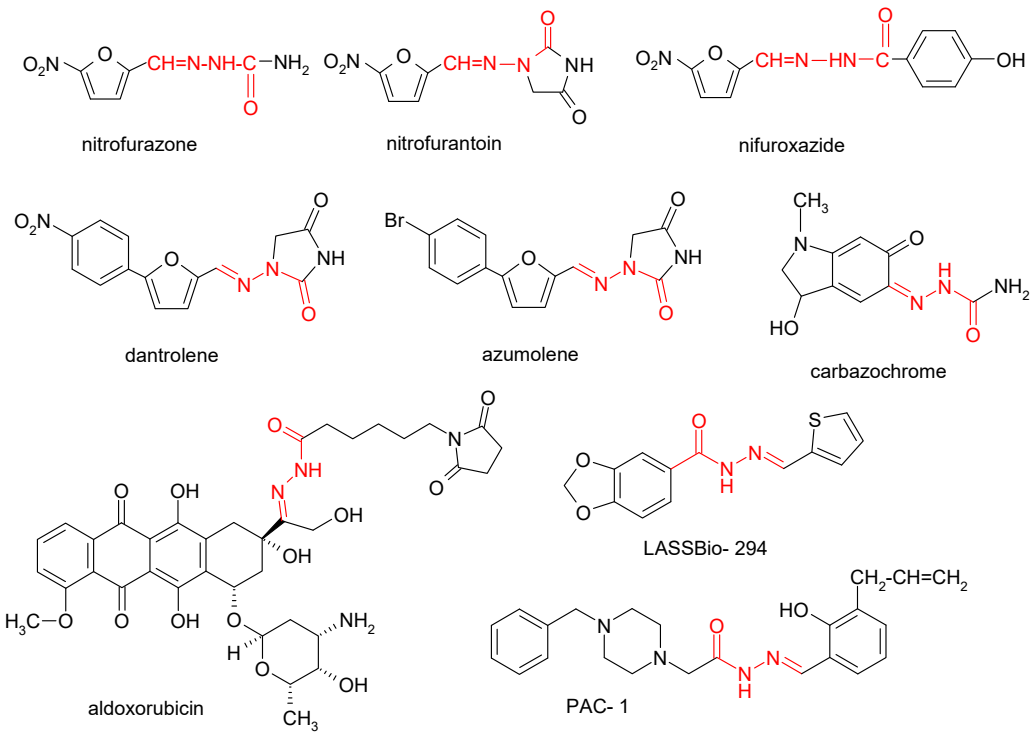

Figure 1. N-acylhydrazone derivatives with biological applications.

 doi:10.20944/preprints202401.1456.v1

When examining compounds containing the NAH fragment, it becomes essential to assess their stability. The stability of these compounds, featuring diverse substituents on the amide nitrogen and the imine carbon, has been investigated. The physicochemical profiles of N-methyl-N-acyl hydrazones exhibit superior stability and water solubility attributed to conformational changes. Another critical factor is the stability of the imine double bond, typically adopting an *E*-type spatial configuration in N-acyl hydrazones, though a *Z*-type configuration is also feasible. In vivo stability studies indicate that interconversion of the C=N bond configuration is not feasible [37].

Numerous investigations have demonstrated the enhanced efficacy of drugs incorporating the NAH fragment compared to the original drug. For example, Effenberger et al. [38] reported that a doxorubicin hybrid, incorporating an N-acyl hydrazone moiety, displayed superior anticancer effects in comparison to unmodified doxorubicin, showcasing a distinct mode of action.

NAH serves as a foundational element for novel anti-inflammatory and analgesic drugs, acting as a pivotal pharmacophore for binding and inhibiting cyclooxygenase (COX). Prolonged use of nonsteroidal anti-inflammatory drugs (NSAIDs) is often hindered by gastrointestinal or cardiovascular complications. Interestingly, certain NSAIDs have demonstrated the capacity to mitigate ulcerogenic effects, attributed to the concealment of the carboxylic acid moiety in these drugs. Consequently, anti-inflammatory and analgesic compounds featuring an NAH moiety are less prone to inducing ulcers compared to NSAIDs lacking this moiety.

In the quest to develop compounds with anti-inflammatory and analgesic properties, along with cardioprotective effects and minimal gastro-toxicity, three pharmacophore fragments derived from NSAID structures (diclofenac, salicylic acid, naproxen, ibuprofen, or ketoprofen), acetylsalicylic acid, and NAH have led to the creation of a new series of NSAID-acyl hydrazone derivatives. Molecular docking studies suggest that these compounds bind to both COX isoforms, exhibiting a higher affinity for COX-2. The inclusion of the NAH subunit reduces gastro-toxicity and ulcer formation without significantly altering the anti-inflammatory efficacy compared to the parent drugs. Notably, the *in vivo* analgesic action of these hybrid compounds generally surpasses that of the parent drugs, making them potential candidates for anti-inflammatory and analgesic drugs with reduced gastro-toxic effects suitable for long-term therapy [39].

Presently, the resistance of pathogenic bacteria to antibiotics employed in therapy is acknowledged as a significant issue posing a threat to public health. Consequently, there is a pressing requirement to formulate novel compounds with varied mechanisms of action to address the escalating danger posed by multidrug-resistant bacteria.

A promising approach has also been shown to be the development of new N-acyl hydrazone derivatives of acridone by condensing acridone acetohydrazide with various aldehydes. The newly synthesized acyl hydrazones underwent *in vitro* testing for their antibacterial efficacy against four human-pathogenic bacterial strains: *Escherichia coli*, *Klebsiella pneumoniae*, *Pseudomonas putida*, and *Staphylococcus aureus*. N-(4-(dimethylamino)benzylidene)-2-(9-oxoacridin-10(9*H*)-yl)acetohydrazide exhibited the highest antibacterial potential against *Pseudomonas putida*, with a minimum inhibitory concentration (MIC) value closely resembling that of chloramphenicol. Additionally, the synthesized compounds underwent docking studies to elucidate their interaction mechanisms with the transcriptional regulatory enzyme of the bacterium *Pseudomonas putida*, as well as with the DNA gyrase of the bacterium *Staphyloccocus aureus*. In summary, the introduction of the acyl hydrazone fragment onto the acridone nucleus demonstrated an enhancement in the antibacterial capacity of the newly synthesized compounds. The results were also supported by molecular docking studies [40].

The prevalence of invasive fungi has markedly increased recently, owing to the growing population susceptible to these infections, the emergence of resistant fungi, and advancements in the diagnosis of such infections. Several existing antifungal medications exhibit a limited range of effectiveness, may lead to resistance, possess potential toxicity, or have the potential for interactions with other drugs. For these reasons, there is a great need for new antifungal drugs, perhaps even some with a novel mechanism of action. Severe fungal infections with a high mortality rate are caused by *Cryptococcus*, *Candida*, *Aspergillus*, and *Pneumocystis* species. Individuals with suppressed immune

Preprints (www.preprints.org) | NOT PEER-REVIEWED | Posted: 19 January 2024 doi:10.20944/preprints202401.1456.v1

systems and those utilizing medical devices like catheters experience a heightened susceptibility to infections.

Previous studies identified an acyl hydrazone, (*E*)-*N*'-(3-bromo-6-hydroxybenzylidene)-2-methylbenzohydrazide (BHBM) that targeted the sphingolipid pathway and showed remarkable antifungal potential. To develop new drugs with antifungal effects, 19 compounds derived from BHBM were tested. Among them, 3 compounds with increased *in vitro* antifungal activity on *Cryptococcus neoformans* and low toxicity were selected. All had antifungal activity superior to BHBM. (*E*)-*N*'-(3,5-dibromo-6-hydroxybenzylidene)-4-bromo-benzohydrazide demonstrated intense activity in animal models against cryptococcosis, candidiasis, and pulmonary aspergillosis, as well as properties appropriate pharmacokinetics and the capability to traverse the blood-brain barrier [41].

Figure 2 presents the medicinal substances with a tuberculostatic activity that contain NAH scaffolds.

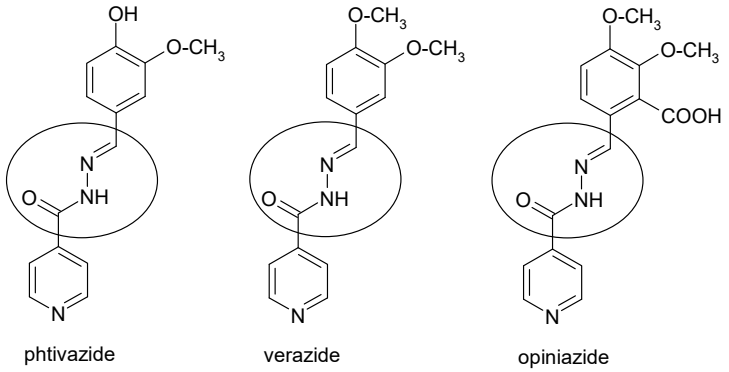

Figure 2. Chemical structure of anti-tuberculosis drugs with NAH pharmacophore moiety.

Owing to the escalating resistance of mycobacteria, there is a demand for innovative classes of antimycobacterial agents featuring novel mechanisms. Some findings in this domain could serve as promising foundations for subsequent studies aimed at developing new lead compounds to address multidrug-resistant tuberculosis.

Six N-acyl hydrazones incorporating vitamin B6 have been successfully synthesized using pyridoxal hydrochloride and N-acyl hydrazine. The characterization of all synthesized compounds has been completed, and their efficacy *against Mycobacterium tuberculosis* has been evaluated. Notably, the N-acyl hydrazone with *para*-pyridine substitution exhibited the most potent activity [42].

Certain N'-benzylidene-2-oxo-2H-chromene-3-carbohydrazides demonstrated noteworthy activity in comparison to first-line drugs like pyrazinamide [14].

New acyl hydrazones based on 2H-chromene or coumarin were synthesized and assessed for their *in vitro* antimycobacterial efficacy against the reference strain *Mycobacterium tuberculosis* H37Rv. Considering the results obtained, these compounds exhibit potential as hybrid anti-tuberculosis agents [43].

Furoxanyl N-acyl hydrazone derivatives, were identified as promising lead compounds for tuberculosis treatment, even against resistant strains. These derivatives displayed activity against a clinical isolate of multidrug-resistant tuberculosis (MDR-TB) strain [44].

From a range of isonicotinoyl hydrazone derivatives, a potential lead compound can be identified for the design and development of more effective antimycobacterial agents. The antimycobacterial results indicated that compounds (*E*)-N'-(2-ethoxybenzylidene) isonicotinohydrazide and (*E*)-N'-(2-fluorobenzyliden) isonicotinohydrazide demonstrated higher effectiveness against *Mycobacterium tuberculosis* H37Rv and two clinical isolates when compared to isoniazid [45].

Novel derivatives of 2-thiophenecarboxylic acid hydrazide were obtained, and among them, 2-thiophenecarbonylhydrazone-5,7-dibromoisatin exhibited the most substantial activity against *M. tuberculosis* H37Rv [46].

Preprints (www.preprints.org) | NOT PEER-REVIEWED | Posted: 19 January 2024 doi:10.20944/preprints202401.1456.v1

New Schiff bases of 4-(1H-pyrrol-1-yl)benzoic acid hydrazide were synthesized and subsequently reacted with copper acetate, leading to the formation of copper complexes. Among these, compounds such as bis[4-(2,5-dimethyl-1*H*-pyrrol-1-yl)-N'-(3,4,5-trimethoxybenzylidene)benzohydrazide] copper (II) anhydride, bis[4-(2,5-dimethyl-1*H*-pyrrol-1-yl)-N'-(3-phenoxybenzylidene)benzohydrazide] copper (II) anhydride, and bis[N'-(2-nitrobenzylidene)-4-(1*H*-pyrrol-1-yl)benzohydrazide] copper (II) anhydride exhibited the highest activity against the *M. tuberculosis* H37Rv strain. Furthermore, these compounds were screened for antibacterial activity and demonstrated notable effectiveness against Gram-negative bacteria [47].

Continuing our research [48-50], through molecular hybridization, we joined two pharmacophore fragments in a single molecule, represented by an NSAID-type carprofen structure and a hydrazone-type structure, obtaining a new series of NSAID-N-acyl hydrazone derivatives (**1a-f**).

2. Results

Six new derivatives of (*EZ*)-N'-benzylidene-(2*RS*)-2-(6-chloro-9*H*-carbazol-2-yl) propanohydrazide have been synthesized according to Scheme 1.

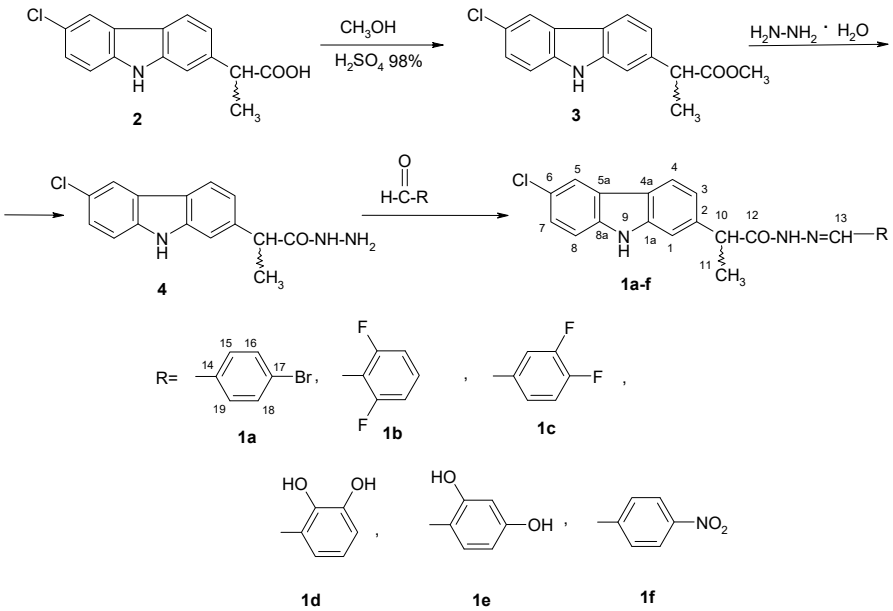

Scheme 1. Synthetic pathway for the novel derivatives of (*EZ*)-N'-benzylidene-(2*RS*)-2-(6-chloro-9*H*-carbazol-2-yl)propanohydrazide.

2.1. Spectral data

The compounds (**1a-f**) contain two geometrical stereoisomers, *E* and *Z*. The superscript s/a represents the alternative between syn- or antiperiplanar conformational stereoisomers, and s+a conveys the distinctive signal for both conformers.

(*EZ*)-N'-(4-bromobenzylidene-(2*RS*)-2-(6-chloro-9*H*-carbazol-2-yl)propane hydrazide (1a); m.p. 215- 222 °C; yield 63 %.

^{1}H-NMR (500 MHz, dmso-d6, δ ppm, J Hz): 11.63 (s, H-9$^{s/a}$); 11.38 (s, H-9$^{s/a}$); 11.37 (s, HN$^{s/a}$); 11.33 (s, HN $^{s/a}$); 8.17 (s, H-13$^{s/a}$); 8.16 (d, H-5 $^{s/a}$, 1.9); 8.13 (d, H-5$^{s/a}$, 1.9); 8.09 (d, H-4$^{s/a}$, 1.8, 8.2); 8.05 (dd, H-4$^{s/a}$, 1.8, 8.2); 7.88 (s, H-13$^{s/a}$); 7.63÷7.61 (m, 4H, H-15, H-19, H-16, H-18); 7.49 (bs, 1H, H-1); 7.46 (d, 1H, H-8, 8.6); 7.34 (m, 1H, H-7); 7.19 (bd, H-3$^{s/a}$, 8.2); 4.81 (q, H-10$^{s/a}$, 7.0); 3.86 (q, H-10$^{s/a}$, 7.0); 1.50 (d, H-11$^{s/a}$, 7.0); 1.47 (d, H-11$^{s/a}$, 7.0) (Figure S1).

^{13}C-NMR(125 MHz, dmso-d6, δ ppm): 175.26 (C-12$^{s/a}$); 170.06 (C-12$^{s/a}$); 145.29 (C-13$^{s/a}$); 141.29 (C-13$^{s/a}$); 140.53 (C-8a^{s+a}); 140.44 (C-1a^{s+a}); 139.37 (C-14a^{s+a}); 138.31 (C-2$^{s/a}$); 138.24 (C-2$^{s/a}$); 133.61 (C-17 $^{s/a}$); 133.55 (C-17 $^{s/a}$); 131.77 (C-16 $^{s/a}$, C18 $^{s/a}$); 131.73 (C-16 $^{s/a}$, C-18 $^{s/a}$); 128.79 (C-15 $^{s/a}$, C-19 $^{s/a}$); 128.54 (C-15 $^{s/a}$, C-19 $^{s/a}$); 125.05 (C-7$^{s/a}$); 124.98 (C-7$^{s/a}$); 123.58 (C-5a^{s+a}); 122.82 (C-4a$^{s/a}$); 122.78 (C-4a$^{s/a}$); 120.41 (C-6$^{s/a}$);

Preprints (www.preprints.org) | NOT PEER-REVIEWED | Posted: 19 January 2024 doi:10.20944/preprints202401.1456.v1

120.18 (C-6$^{s/a}$); 119.68 (C-5$^{s/a}$); 119.60 (C-5$^{s/a}$); 119.55 (C-4$^{s/a}$); 119.47 (C-4$^{s/a}$); 119.03 (C-3$^{s/a}$); 118.76 (C-3$^{s/a}$); 112.31 (C-8$^{s/a}$); 112.25 (C-8$^{s/a}$); 109.84 (C-1$^{s/a}$); 109.61 (C-1$^{s/a}$); 44.57 (C-10$^{s/a}$); 41.26 (C-10$^{s/a}$); 19.01 (C-11$^{s/a}$); 18.96 (C-11$^{s/a}$) (Figure S2).

FT-IR (ATR in solid, ν cm-1): 3409m; 3241m; 3046w; 2978w; 1659vs; 1621sh; 1598w; 1535m; 1470m; 1346m; 1273w; 1229m; 1186m; 1063m; 1006w; 948w; 867w; 816m; 727w.

Chemical Formula $C_{22}H_{17}BrClN_3O$, Exact Mass 453.02435, **HRMS** (APCI+, DMSO+MeOH), m/z (%): 456.02927 (100) [M+H]+, 228.05769 (79) [$C_{14}H_{11}ClN$]+ (Figure S3, S4).

(*EZ*)-N'-(2,6-difluorobenzylidene-(2*RS*)-2-(6-chloro-9*H*-carbazol-2-yl)propane hydrazide (1b); m.p. 214- 221 °C; yield 68 %

For **1b** compound the *E* / *Z* ratio is 1.0 : 0.67.

^{1}H-NMR(500 MHz, dmso-d6, δ ppm, *J* Hz): 11.70 (s, H-9$^{s/a}$); 11.39 (s, H-9$^{s/a}$); 11.45 (s, HN$^{s/a}$); 11.34 (s, HN$^{s/a}$); 8.35 (s, H-13$^{s/a}$); 8.19 (s, H-13$^{s/a}$); 8.17 (d, H-5$^{s/a}$, 1.9); 8.13 (d, H-5$^{s/a}$, 1.9); 8.09 (d, H-4$^{s/a}$, 8.2); 8.05 (d, H-4$^{s/a}$, 8.2); 7.49 (tt, 1H, H-17, *J*(H^{17}-F^{15,19})=6.6 Hz, *J*(H^{17}-H^{16,18})=9.1 Hz); 7.46 (d, 1H, H-8$^{s/a}$, 8.6); 7.44 (bs, 1H, H-1$^{s/a}$); 7.36 (dd, 1H, H-7$^{s/a}$, 1.9, 8.6); 7.34 (dd, 1H, H-7$^{s/a}$, 1.9, 8.6); 7.22÷7.14 (m, 2H, H-3, H-16, H-18); 4.79 (q, H-10$^{s/a}$, 7.0); 3.84 (q, H-10$^{s/a}$, 7.0); 1.49 (d, H-11$^{s/a}$, 7.0); 1.47 (d, H-11$^{s/a}$, 7.0).

H-1, H-8 and H-17 protons can appear together and are difficult to identify, presenting as a multiplet in the area 7.52÷7.43 (m, 3H, H-1, H-8, H-17);

The isomer with H-10 at δ= 4.79 ppm is the majority compared to the isomer with δ = 3.84 ppm; ratio 1/0.67 (Figure S5).

^{13}C-NMR (125 MHz, dmso-d6, δ ppm): 175.28 (C-12$^{s/a}$); 169.90 (C-12$^{s/a}$); 160.27 (dd, C-15$^{s/a}$ or C-19$^{s/a}$, ^4J(F^{15}-F^{19})=6 Hz, *J*(C-F)=254.3 Hz); 160.19 (dd, C-15$^{s/a}$ or C-19$^{s/a}$, ^4J(F^{15}-F^{19})=6 Hz, *J*(C-F)=248.1 Hz); 140.57 (C-8a$^{s/a}$); 140.51 (C-8a$^{s/a}$); 139.97 (C-1a$^{s/a}$); 139.94 (C-1a$^{s/a}$); 138.33 (C-2$^{s/a}$); 138.27 (C-2$^{s/a}$); 136.94 (d, C-13$^{s/a}$, *J*(2F^{15,19}-C^{13}) =14.6 Hz); 132.90 (d, C-13$^{s/a}$, *J*(2F^{15,19}-C^{13})=14.6 Hz); 131.66 (t, C-17$^{s/a}$, ^3J(2F-C^{17})=11.1 Hz); 131.40 (t, C-17$^{s/a}$, ^3J(2F-C^{17})=11.1 Hz); 125.08 (C-7$^{s/a}$); 124.99 (C-7$^{s/a}$); 123.59 (C-5a^{s+a}); 122.83 (C-4a$^{s/a}$); 122.75 (C-4a$^{s/a}$); 120.47 (C-5$^{s/a}$); 120.46 (C-6$^{s/a}$); 120.30 (C-5$^{s/a}$); 120.28(C-6$^{s/a}$); 119.61 (C-3$^{s/a}$); 119.50 (C-3$^{s/a}$); 112.40 (dd, C-16$^{s/a}$ and C-18$^{s/a}$, ^4J(F^{19}-C^{16})=4.2 Hz, ^{vic}J(F^{19}-C^{16})=15.4 Hz); 112.25 (dd, C-16$^{s/a}$ and C-18$^{s/a}$, ^4J(F^{19}-C^{16}) =4.2 Hz, ^{vic}J(F^{19}-C^{16})=15.4 Hz); 120.27 (C-4^{s+a}); 112.26 (C-8^{s+a}); 111.44 (t, C-14^{s+a}, ^{vic}J(2F-C^{14})=14 Hz); 109.86 (C-1$^{s/a}$); 109.66 (C-1$^{s/a}$); 44.59 (C-10$^{s/a}$); 40.65 (C-10$^{s/a}$); 18.87 (C-11$^{s/a}$); 18.67 (C-11$^{s/a}$) (Figure S6).

From simulations results that ^{vic}J(F15-C16)=21.2 Hz; 4J(F19-C16)=4.2 Hz.

FT-IR (ATR in solid, ν cm-1): 3327s; 3242sh; 3037m; 2978w; 2926w; 1633vs; 1617sh; 1592vs; 1464vs; 1385m; 1348m; 1240s; 1207sh; 1066m; 1028w; 1000s; 956m; 863w; 791m.

Chemical Formula $C_{22}H_{16}ClF_2N_3O$, Exact Mass 411.09500, **HRMS** (APCI+, DMSO+MeOH), m/z (%): 412.10269 (100) [M+H]+, 228.05814 (12) [C14H11ClN]+, 191.14304 (7), 158.02701 (6), 141.00042 (10), 77.03822 (5) (Figure S7, S8).

(*EZ*)-N'-(3,4-difluorobenzylidene-(2*RS*)-2-(6-chloro-9*H*-carbazol-2-yl)propane hydrazide (1c); m.p. 224- 230 °C; yield 65 %.

For compound **1c** the ratio between E / Z stereoisomers is 1.0 : 0.9.

^{1}H-NMR (500 MHz, dmso-d6, δ ppm, J Hz): 11.67 (s, H-9$^{s/a}$); 11.38 (s, HN^{s+a}); 11.33 (s, H-9$^{s/a}$); 8.18 (s, H-13$^{s/a}$); 8.16 (d, H-5$^{s/a}$, 1.8); 8.13 (d, H-5$^{s/a}$, 1.8); 8.09 (d, H-4$^{s/a}$, 8.2); 8.06 (d, H-4$^{s/a}$, 8.2); 7.87 (s, H-13$^{s/a}$); 7.74 (m, 1H, H-15$^{s/a}$); 7.68 (m, 1H, H-15$^{s/a}$); 7.51-7.44 (m, 4H, H-1, H-8, H-18, H-19); 7.35 (dd, H-7$^{s/a}$, 1.8, 7.6); 7.33 (dd, H-7$^{s/a}$, 1.8, 7.6); 7.20 (d, H-3$^{s/a}$, 8.2); 7.18 (d, H-3$^{s/a}$, 8.2); 4.83 (q, H-10$^{s/a}$, 7.0); 3.86 (q, H-10$^{s/a}$, 7.0); 1.49 (d, H-11$^{s/a}$, 7.0); 1.47 (d, H-11$^{s/a}$, 7.0) (Figure S9).

^{13}C-NMR (125 MHz, dmso-d6, δ ppm): 175.26 (C-12$^{s/a}$); 170.03 (C-12$^{s/a}$); 150.19 (dd, C-16, J(C^{16}-F^{17})=13.8 Hz, J(C^{16}-F^{16})=248.8 Hz); 149.73 (dd, C-17, J(C^{16}-F^{17})=15.0 Hz, J(C^{17}-F^{17})=245 Hz); 144.34 (C-13$^{s/a}$); 140.56 (C-8a^{s+a}); 140.23 (C-13$^{s/a}$); 139.85 (C-1a^{s+a}); 138.32 (C-2$^{s/a}$); 138.25 (C-2$^{s/a}$); 132.20 (C-14$^{s/a}$, J(C^{14}-F^{16})=5.7 Hz); 132.12 (C-14$^{s/a}$, J(C^{14}-F^{16})=5.7 Hz); 125.06 (C-7$^{s/a}$); 124.96 (C-7$^{s/a}$); 124.11 (C-19$^{s/a}$); 124.00 (C-19$^{s/a}$); 123.58 (C-5a^{s+a}); 122.83 (C-4a$^{s/a}$); 122.77 (C-4a$^{s/a}$); 120.18 (C-6$^{s/a}$); 120.53 (C-4^{s+a}); 119.68 (C-6$^{s/a}$); 119.67 (C-5$^{s/a}$); 119.55 (C-5$^{s/a}$); 119.04 (C-3$^{s/a}$); 118.74 (C-3$^{s/a}$); 118.03 (d, C-18$^{s/a}$, J(C^{18}-F^{17})=14.8 Hz); 117.99 (d, C-18$^{s/a}$, J(C^{18}-F^{17})=14.8 Hz); 117.96 (d, C-18$^{s/a}$, J(C^{18}-F^{17}); 115.24 (d, C-15$^{s/a}$, J(C^{15}-F^{16})= 19.5 Hz); 114.85 (d, C-15$^{s/a}$, J(C^{15}-F^{16})=19.5 Hz); 112.32 (C-8$^{s/a}$); 112.25 (C-8$^{s/a}$); 109.72 (C-1$^{s/a}$); 109.62 (C-1$^{s/a}$); 44.44 (C-10$^{s/a}$); 41.12 (C-10$^{s/a}$); 18.97 (C-11$^{s/a}$); 18.88 (C-11$^{s/a}$) (Figure S10).

FT-IR (ATR in solid, ν cm-1): 3348m; 3190w; 3028m; 2912w; 1644vs; 1577s; 1514s; 1466m; 1444m; 1349m; 1279s; 1242m; 1204s; 1065m; 946w; 866w; 811m; 727w; 624m; 594m.

Chemical Formula $C_{22}H_{16}ClF_2N_3O$, Exact Mass 411.09500, **HRMS** (APCI+, DMSO+MeOH), m/z (%): 412.10001 (100) [M+H]+, 328.11961 (18) [C18H19ClN3O]+, 228.05638 (13) [C14H11ClN]+ (Figure S7, S8) (Figure S11, S12).

(*EZ*)-N'-(2,3-dihydroxybenzylidene-(2*RS*)-2-(6-chloro-9H-carbazol-2-yl) propane hydrazide (1d); m.p. 143- 149 °C; yield 70 %

In compound **1d**, stereoisomers E and Z are in a ratio of 1.0 : 0.35.

^{1}H-NMR (300 MHz, dmso-d6, δ ppm, J Hz): 11.79 (s, H-9 $^{s/a}$); 11.27 (s, H-9 $^{s/a}$); 11.38 (s, HN $^{s/a}$); 11.34 (s, HN $^{s/a}$); 10.95 (bs, OH); 9.46 (bs, OH); 9.19 (bs, OH); 8.35 (s, H-13 $^{s/a}$); 8.21 (s, H-13 $^{s/a}$); 8.17 (d, H-5 $^{s/a}$, 1.9); 8.14 (d, H-5 $^{s/a}$, 1.9); 8.10 (d, H-4 $^{s/a}$, 8.2); 8.06 (d, H-4$^{s/a}$, 8.2); 7.49-7.44 (m, 2H, H-1, H-8); 7.34 (dd, H-7 $^{s/a}$, 1.9, 7.6); 7.33 (dd, H-7 $^{s/a}$, 1.9, 7.6); 7.19 (d, H-3$^{s/a}$, 8.2); 7.17 (d, H-3$^{s/a}$, 8.2); 6.89 (dd, 1H, H-19$^{s/a}$); 6.81 (dd, H-17$^{s/a}$, 1.7, 7.8); 6.80 (dd, H-17$^{s/a}$, 1.7, 7.8); 6.70 (t, 1H, H-18$^{s/a}$, 7.8); 4.72 (q, H-10$^{s/a}$, 7.0); 3.86 (q, H-10 $^{s/a}$, 7.0); 1.50 (d, H-11 $^{s/a}$, 7.0); 1.46 (d, H-11 $^{s/a}$, 7.0) (Figure S13).

^{13}C-NMR (75 MHz, dmso-d6, δ ppm): 174.64 (C-12$^{s/a}$); 169.68 (C-12$^{s/a}$); 147.83 (C-13$^{s/a}$); 145.93 (C-14$^{s/a}$); 145.58 (C-14$^{s/a}$); 145.55 (C-15$^{s/a}$); 145.13 (C-15$^{s/a}$); 141.41 (C-13$^{s/a}$); 140.55 (C-8a$^{s/a}$); 140.37 (C-8a$^{s/a}$); 139.83 (C-1a^{s+a}); 138.33 (C-2$^{s/a}$); 138.27 (C-2$^{s/a}$); 125.08 (C-7$^{s/a}$); 124.98 (C-7$^{s/a}$); 123.61 (C-5a$^{s/a}$); 123.58 (C-5a$^{s/a}$); 122.85 (C-4a$^{s/a}$); 122.76 (C-4a$^{s/a}$); 120.47 (C-6$^{s/a}$); 120.46 (C-16$^{s/a}$); 120.21 (C-6$^{s/a}$); 120.20 (C-16$^{s/a}$); 119.87 (C-5$^{s/a}$); 119.86 (C-4$^{s/a}$); 119.71 (C-4$^{s/a}$); 119.70 (C-5$^{s/a}$); 119.05 (C-19$^{s/a}$); 119.00 (C-19$^{s/a}$); 118.99 (C-3$^{s/a}$); 118.80 (C-18$^{s/a}$); 118.75 (C-3$^{s/a}$); 117.27 (C-17$^{s/a}$); 117.08 (C-17$^{s/a}$); 112.35 (C-8$^{s/a}$); 112.32 (C-8$^{s/a}$); 109.63 (C-1$^{s/a}$); 44.37 (C-10$^{s/a}$); 41.28 (C-10$^{s/a}$); 19.14 (C-11$^{s/a}$); 18.90 (C-11$^{s/a}$) (Figure S14).

FT-IR (ATR in solid, ν cm-1): 3370m; 3185w; 3043w; 2972w; 2933w; 1642vs; 1555m; 1468s; 1359m; 1266vs; 1198s; 1118m; 1067m; 1007w; 945m; 869w; 761w; 729m; 611m.

Chemical Formula $C_{22}H_{18}ClN_3O_3$, Exact Mass 407.10367, **HRMS** (APCI+, DMSO+MeOH), m/z (%): 408.11007 (100) [M+H]+, 328.12057 (5) [C18H19ClN3O]+ (Figure S15, S16).

(*EZ*)-N'-(2,4-dihydroxybenzylidene-(2*RS*)-2-(6-chloro-9*H*-carbazol-2-yl)propanehydrazide (1e), m.p. 170- 175 °C; yield 63 %

For compound **1e** the ratio between the geometric stereoisomers E / Z is 1.0 : 3.0.

^{1}H-NMR (300 MHz, dmso-d6, δ ppm, J Hz): 11.60 (s, H-9$^{s/a}$); 11.35 (s, H-9$^{s/a}$); 11.37 (s, HN$^{s/a}$); 11.29 (s, HN$^{s/a}$); 11.09 (bs, OH); 10.01 (bs, OH); 9.92 (bs, OH); 9.9.80 (bs, OH); 8.26 (s, H-13$^{s/a}$); 8.16 (d, H-5$^{s/a}$, 1.9); 8.13 (d, H-5$^{s/a}$, 1.9); 8.09 (d, H-4 $^{s/a}$, 8.2); 8.08 (s, H-13$^{s/a}$); 8.06 (d, H-4$^{s/a}$, 8.2); 7.49-7.45 (m, 2H, H-1, H-8); 7.45 (d, 1H, H-19 $^{s/a}$, 8.4); 7.35 (dd, H-7$^{s/a}$, 1.9, 7.6); 7.33 (dd, H-7 $^{s/a}$, 1.9, 7.6); 7.24 (d, 1H, H-19 $^{s/a}$, 8.4); 7.19 (d, H-3$^{s/a}$, 8.2); 7.16 (d, H-3$^{s/a}$, 8.2); 6.32 (dd, 1H, H-18 $^{s/a}$, 1.9, 8.4); 6.28 (d, 1H, H-16 $^{s/a}$, 1.9); 4.65 (q, H-10$^{s/a}$, 7.0); 3.83 (q, H-10 $^{s/a}$, 7.0); 1.49 (d, H-11 $^{s/a}$, 7.0); 1.44 (d, H-11 $^{s/a}$, 7.0) (Figure S17).

^{13}C-NMR (75 MHz, dmso-d6, δ ppm): 174.15 (C-12$^{s/a}$); 169.27 (C-12$^{s/a}$); 160.67 (C-15 $^{s/a}$); 160.56 (C-15$^{s/a}$); 159.28 (C-17$^{s/a}$); 157.96 (C-17$^{s/a}$); 148.02 (C-13$^{s/a}$); 142.15 (C-13$^{s/a}$); 140.56 (C-8a$^{s/a}$); 140.48 (C-8a$^{s/a}$); 140.00 (C-1a^{s+a}); 138.32 (C-2$^{s/a}$); 138.27 (C-2$^{s/a}$); 131.07 (C-19$^{s/a}$); 128.63 (C-19$^{s/a}$); 125.04 (C-7$^{s/a}$); 124.95 (C-7$^{s/a}$); 123.62 (C-14^{s+a}); 122.85 (C-4a$^{s/a}$); 122.77 (C-4a$^{s/a}$); 120.42 (C-6$^{s/a}$); 120.41 (C-4$^{s/a}$); 120.18 (C-6$^{s/a}$); 120.17 (C-4$^{s/a}$); 119.47 (C-5$^{s/a}$); 119.54 (C-5$^{s/a}$); 118.91 (C-3$^{s/a}$); 118.76 (C-3$^{s/a}$); 112.32 (C-8$^{s/a}$); 112.24 (C-8$^{s/a}$); 109.65 (C-1$^{s/a}$); 109.60 (C-1$^{s/a}$); 107.85 (C-18$^{s/a}$); 107.58 (C-18$^{s/a}$); 102.57 (C-16$^{s/a}$); 102.35 (C-16$^{s/a}$); 44.26 (C-10$^{s/a}$); 41.32 (C-10$^{s/a}$); 19.23 (C-11$^{s/a}$); 18.89 (C-11$^{s/a}$) (Figure S18).

FT-IR (ATR in solid, ν cm-1): 3356m; 3224m; 3056w; 2980w; 1645vs; 1619vs; 1541sh; 1508s; 1445s; 1320m; 1227s; 1161m; 1116m; 1068m; 963m; 808m; 754m; 650w.

Chemical Formula $C_{22}H_{18}ClN_3O_3$, Exact Mass 407.10367, **HRMS** (APCI+, DMSO+MeOH), m/z (%): 408.11047 (100) [M+H]+, 228.05774 (3) [C14H11ClN]+ (Figure S19, S20).

(*EZ*)-N'-(4-nitrobenzylidene-(2*RS*)-2-(6-chloro-9*H*-carbazol-2-yl) propane hydrazide (1f); m.p. 235,6- 238 °C; yield 74 %

The ratio between E and Z is 1.0:0.85.

^{1}H-NMR (500 MHz, dmso-d6, δ ppm, J Hz): 11.87(s, H-9$^{s/a}$); 11.61(s, H-9$^{s/a}$); 11.39(s, HN$^{s/a}$); 11.35(s, HN$^{s/a}$); 8.26(s, H-13$^{s/a}$); 7.99(s, H-13$^{s/a}$); 8.28(d, 2H, H-16$^{s/a}$, H-18 $^{s/a}$, 9.8); 8.26(d, 2H, H-16$^{s/a}$, H-18 $^{s/a}$, 9.8); 7.94(d, 2H, H-15$^{s/a}$, H-19 $^{s/a}$, 9.8); 7.91(d, 2H, H-15$^{s/a}$, H-19 $^{s/a}$, 9.8); 8.17(d, H-5$^{s/a}$, 1.9); 8.13(d, H-5$^{s/a}$, 1.9); 8.10(d, H-4 $^{s/a}$, 8.2); 8.06(d, H-4$^{s/a}$, 8.2); 7.48(bs, 1H, H-1^{s+a}); 7.47(d, 1H, H-8$^{s/a}$, 8.5); 7.45(d,

Preprints (www.preprints.org) | NOT PEER-REVIEWED | Posted: 19 January 2024 doi:10.20944/preprints202401.1456.v1

1H, H-8 $^{s/a}$, 8.5); 7.35(dd, 1H, H-7$^{s/a}$, 1.9, 8.5);); 7.33(dd, 1H, H-7$^{s/a}$, 1.9, 8.5); 7.20(d, H-3$^{s/a}$, 8.2); 7.18(d, H-3$^{s/a}$, 8.2);4.83(q, H-10$^{s/a}$, 7.0); 3.90(q, H-10$^{s/a}$, 7.0); 1.50(d, H-11$^{s/a}$, 7.0); 1.47(d, H-11$^{s/a}$, 7.0) (Figure S21).

^{13}C-NMR (125 MHz, dmso-d6, δ ppm): 175.48(C-12$^{s/a}$); 170.33(C-12$^{s/a}$); 147.74(C-17$^{s/a}$); 147.53(C-17$^{s/a}$); 140.66(C-8a$^{s/a}$); 140.62(C-8a$^{s/a}$); 140.54(C-1a^{s+a}); 140.30(C-2$^{s/a}$); 139.79(C-2$^{s/a}$); 138.31(C-14$^{s/a}$); 138.25(C-14$^{s/a}$); 123.70(C-5a^{s+a}); 122.84(C-4a$^{s/a}$); 122.78(C-4a$^{s/a}$); 120.46(C-6$^{s/a}$); 120.23(C-6$^{s/a}$); 144.12(C-13$^{s/a}$); 140.15(C-13$^{s/a}$); 127.84(C-15$^{s/a}$, C-19$^{s/a}$); 127.57(C-15$^{s/a}$, C-19$^{s/a}$); 124.02(C-16^{s+a}, C-18 $^{s+a}$); 125.10(C-7$^{s/a}$); 125.01C-7$^{s/a}$); 120.64(C-6$^{s/a}$); 120.54(C-6$^{s/a}$); 119.69(C-5$^{s/a}$); 119.65(C-5$^{s/a}$); 118.93(C-3$^{s/a}$); 118.74(C-3$^{s/a}$); 112.33(C-8$^{s/a}$); 112.28(C-8$^{s/a}$); 109.92(C-1$^{s/a}$); 109.65(C-1$^{s/a}$); 44.54(C-10$^{s/a}$); 41.35(C-10$^{s/a}$); 18.90(C-11^{s+a}) (Figure S22).

FT-IR (ATR in solid, ν cm-1): 3411w; 3313w; 3235w; 3048w; 2896w; 1655s; 1583m; 1555m; 1519vs; 1462m; 1342vs; 1273m; 1236m; 1192m; 1099w; 1068w; 950w; 844m; 737w.

Chemical Formula $C_{22}H_{17}ClN_4O_3$, Exact Mass 420.09892, **HRMS** (APCI+, DMSO+MeOH), m/z (%): 421.10635 (70) [M+H]+, 391.13232 (6), 328.12149 (100) $[C_{18}H_{19}ClN_3O]$+, 296.25864 (49), 282.27930 (15), 228.05769 (8) $[C_{14}H_{11}ClN]$+, 79.02095 (9) (Figure S23, S24).

2.2. Tuberculostatic activity

At the concentration of 4 mg/mL, the examined compounds demonstrated a greater inhibitory effect compared to 2 mg/mL. Among the tested compounds, **1b**, **1d**, and **1e** emerged as the most potent agents, effectively inhibiting the growth of all four strains of M. tuberculosis, whether susceptible or resistant, at 4 mg/mL. Particularly noteworthy was the efficacy of compound **1c**, which hindered the growth of three out of the four tested strains, including the M. tuberculosis strain resistant to INH. The lowest antimycobacterial activity has been noted for the compound **1a** (Table 2).

Table 2. The count of M. tuberculosis colonies per standard inoculum volume (0.2 mL) retrieved from the culture medium supplemented with varying concentrations of the tested substances.

Mycobacterial strain	Tested compound	2 mg/mL	4 mg/mL	RIF	INH
***M. tuberculosis* 2327**	**1a**	30	30	<20	<20
	1b	30-100	30-100	<20	<20
	1c	30	30	<20	<20
	1d	30	30	<20	<20
	1e	30-100	30	<20	<20
	1f	30-100	30-100	<20	<20
***M. tuberculosis* 2337**	**1a**	30-100	30	<20	<20
	1b	30-100	30	<20	<20
	1c	30	30	<20	<20
	1d	30	30	<20	<20
	1e	30-100	30	<20	<20
	1f	30-100	30-100	<20	<20
***M. tuberculosis* 1762**	**1a**	30-100	30-100	<20	>20
	1b	30-100	30	<20	>20
	1c	30-100	30	<20	>20
	1d	30-100	30	<20	>20
	1e	30-100	30	<20	>20
	1f	>100	30-100	<20	>20
***M. tuberculosis* 309**	**1a**	30-100	30-100	>20	>20
	1b	30-100	30	>20	>20
	1c	30-100	30-100	>20	>20
	1d	30-100	30	>20	>20
	1e	30-100	30	>20	>20
	1f	>100	30-100	>20	>20

Preprints (www.preprints.org) | NOT PEER-REVIEWED | Posted: 19 January 2024 doi:10.20944/preprints202401.1456.v1

3. Discussion

For the production of N-acyl hydrazones, we employed a microwave-assisted synthesis method. This approach offers advantages such as reduced reaction time, increased reaction yield, and enhanced purity of the final products by minimizing undesired side reactions when compared to conventional heating methods.

The analysis of NMR spectra confirms the existence of multiple signals due to geometrical stereoisomers *E* and *Z* or conformational stereoisomers synperiplanar and antiperiplanar found in the mixture. The presence of the chiral center at C-10 can double the number of diastereoisomers. For the N-acyl hydrazone group, -CO-NH-N=CH-, in 1H NMR spectra, -NH- gave a signal (singlet) at 11.38 ppm (for compound 1c, as a unique signal) or showed two singlet signals for the other compounds, between 11.37- 11.45 and 11.29- 11.35 ppm for *syn* or *anti* stereoisomers. The proton of =CH- moiety showed a singlet signal between 8.17- 8.35 ppm and 7.87- 8.21 ppm as an alternative between *syn* or *anti* stereoisomers for each compound. In carbon spectra, the signals of C12 and C13 exhibit doubling owing to the presence of *syn*/*anti*-conformational stereoisomerism. Thus, for the acyl hydrazone group, ^{13}C NMR spectra showed signals between 174.15- 175.48 and 169.27- 170.33 ppm due to C12 and between 136.94- 148.02 and 132.90- 142.15 ppm for C13.

The APCI+ high-resolution mass spectra were obtained using a mixture of DMSO+MeOH. The [M+H]+ molecular peaks were identified as base peaks for five substances, while the mass spectrum of 1f was observed with a relative intensity of 70 %. The presence of the molecular peaks as base peaks or with high relative intensity in the case of 1f is evidence of the compounds' identity and purity. The additional peaks identified in the mass spectra of the compounds align with the $[C_{18}H_{19}ClN_3O]$+ and $[C_{14}H_{11}ClN]$+ cations at calculated m/z values of 328.12112 and 228.05800, for which the proposed structures are depicted on Figure 3. The two methyl groups attached in the fragment at a calculated m/z of 328.12112 probably result from the measurement in a methanolic solution.

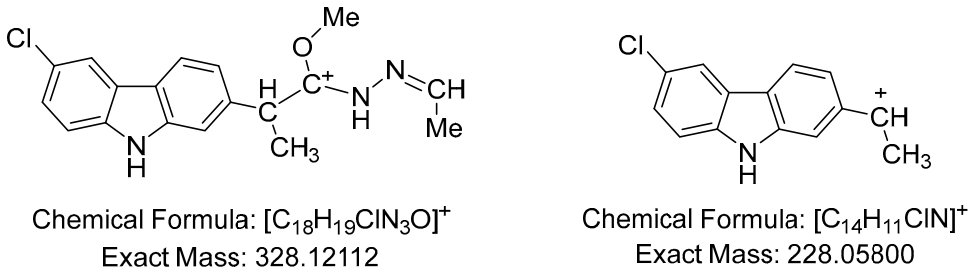

Figure 3. $[C_{18}H_{19}ClN_3O]^+$ and $[C_{14}H_{11}ClN]^+$ cations.

M. tuberculosis infection is still prevalent at the global level, infecting ~one-third of the world's population. and representing one of the top causes of infection-related mortality, with ~29% of deaths being correlated to its resistance to currently available drugs [51-55]. Many factors, such as late diagnosis, inappropriate treatment selection, drug supply and/or drug concentration, and poor patient compliance, have played a role in the rise of strains exhibiting multiple drug resistance (MDR), extensive drug resistance (XDR), extremely drug resistance (XXDR), or, in some cases, totally drug resistance (TDR) [56-59]. This threatening context requires the urgent development of novel therapeutic strategies to reduce the mortality and morbidity burden and get one step closer to the aim of the World Health Organization (WHO) to achieve a 95% decrease in mortality due to *M. tuberculosis* infection. and a 90% decrease in new cases by 2035 [60]. Several new antibiotics (bedaquiline, delamanid, and pretomanid) have received approval for the treatment of *M. tuberculosis* MDR infections [51,61], but unfortunately, resistance has already merged with these new compounds [62,63]. Derivatives of existing anti-tuberculosis medications such as ethambutol, or repurposed drugs such as linezolid and clofazimine have also been proposed but threatened by the quick emergence of resistance [57,63-65]. Numerous other compounds have demonstrated efficacy through

 doi:10.20944/preprints202401.1456.v1

both *in vitro* and *in vivo* studies [66-76], but further research is needed to confirm their efficiency and mechanisms of action before advancing to clinical trials.

To tackle this challenge, we have integrated two pharmacophore fragments into a single molecule, comprising an NSAID-type carprofen structure and a hydrazone-type structure. This resulted in a novel series of NSAID-N-acyl hydrazone derivatives, which were then assessed for their tuberculostatic activity. The compounds were tested for their effectiveness against four microbial strains with varying susceptibility profiles to RIF and INH.

The most active compounds were those bearing two fluorine or hydroxy substituents on the benzylidene fragment. Thus, 1b, 1d, and 1e harbored two fluorine atoms (in positions 2, 6) or two hydroxy groups (in positions 2, 3, and 2, 4, respectively) on the benzylidene fragment. The 1c compound, which also bears two fluorine atoms on the benzylidene fragment but in positions 3, 4 was less active than 1b. This implies the significance of the positioning of identical substituents concerning the rest of the molecule and in relation to each other for the activity of these compounds, especially against the MDR strains. The lowest antimycobacterial activity has been noted for the compounds 1a and 1f, bearing only one substituent on the benzylidene fragment situated in the *para* position.

4. Materials and Methods

4.1. Measurements

All reagents were obtained from Merck (Darmstadt, Germany) or Aldrich (Steinheim, Germany). The microwave-assisted synthesis was carried out using a Biotage® Initiator Classic 2.0 system (Biotage, Uppsala, Sweden).

Melting points were determined using an Electrothermal 9100 apparatus (Bibby Scientific Ltd, Stone, UK) in open capillary tubes and were not corrected.

The IR spectra were conducted on a Bruker Vertex 70 FT-IR spectrometer (Bruker Corporation, Billerica, MA, USA). Frequencies are expressed per cm^{-1} and were obtained using the ATR technique, denoted as w (weak band), m (medium band), s (intense band), and vs (very intense band).

The ^{1}H NMR and ^{13}C NMR spectra were recorded in deuterated dimethyl sulfoxide (dmso-d6) using a Bruker Fourier 300 MHz instrument (Bruker Corporation, Billerica, MA, USA), operating at 300 MHz for ^{1}H NMR and at 75 MHz for ^{13}C NMR. Additionally, a Bruker Avance III 500 MHz instrument (Bruker Corporation, Billerica, MA, USA) was employed, operating at 500 MHz for proton and 125 MHz for carbon. In NMR spectra, chemical shifts were recorded as δ values in parts per million (ppm) relative to tetramethylsilane as an internal standard. Coupling constants (J) were reported in Hertz. Signal multiplicities were indicated as singlet (s), broad singlet (bs), doublet (d), broad doublet (bd), triplet (t), quartet (q), doublet of doublet (dd), and multiplet (m). The ^{1}H NMR data were presented in the following order: chemical shifts, multiplicity, signal/atom attribution, and coupling constants. For ^{13}C NMR data, the order was chemical shifts and signal/atom attribution.

The APCI+ high-resolution mass spectra for compounds **1a-f** were recorded on a Thermo Scientific LTQ-Orbitrap XL spectrometer equipped with a standard ESI/APCI source. Thermo Xcalibur software (XcaliburTM Software, Thermo Fisher Scientific, Waltham, MA USA) was utilized for processing the mass spectra.

4.2. Chemistry

The syntheses of the compounds methyl (2*RS*)-2-(6-chloro-9*H*-carbazol-2-yl)-propanoate (carprofen methyl ester) (**3**) and (2*RS*)-2-(6-chloro-9*H*-carbazol-2- yl) propane hydrazides (carprofen hydrazides) (**4**) were presented in a previously published article [48].

For the synthesis of (*EZ*)-N'-benzylidene-(2*RS*)-2-(6-chloro-9*H*-carbazol-2-yl)propanohydrazide derivatives (**1a-f**), (2*RS*)-2-(6-chloro-9*H* -carbazol-2-yl)propanohydrazide (**4**) (0.001mol) and various aromatic aldehydes (0.001mol), in 3 mL of absolute methanol and four drops of the catalyst, glacial acetyl acid, are introduced into a microwave tube. The reaction mixture undergoes pre-stirring for 5 minutes, followed by irradiation for 25 minutes at 90 °C with very high absorption. Once the

 doi:10.20944/preprints202401.1456.v1

designated time elapses, the mixture is cooled to room temperature and refrigerated overnight. The resulting product is then filtered and subjected to recrystallization from a 1:2 mixture of isopropanol and water.

The compounds exhibit solubility at room temperature in pyridine, DMSO, and DMF, while they are soluble when heated in lower alcohols, acetone, chloroform, benzene, toluene, xylene, 1,4-dioxane, and ethyl acetate. However, they remain insoluble in water, hexane, and methylene chloride.

4.3. Tuberculostatic activity assay

The tuberculostatic activity was evaluated against four strains of *M. tuberculosis*, including two susceptible to rifampicin (RIF) and isoniazid (INH) (encoded 2327 and 2337), one susceptible to RIF but resistant to INH (encoded 1762), and one resistant to both RIF and INH (encoded 309). The tested substances were incorporated into Lowenstein Jensen (LJ) solid medium at concentrations of 2 and 4 mg/ml. The tubes were then incubated at a 45° angle at 37°C to ensure even distribution of the tested substances in the culture medium. After 48 hours, the inoculum was seeded onto the respective tubes, and incubation continued for 28 days.

For the sterility control of the culture medium and tested substances, LJ tubes supplemented with compounds **1a-f** at concentrations of 2 mg/ml and 4 mg/ml were left unseeded in the thermostat at 37°C and observed for 28 days to confirm the absence of growth or contamination. The inoculum was seeded on LJ tubes and used as positive controls.

The colonies that emerged on the media containing varying concentrations of the tested substance were counted after an incubation period of 28 days.

For RIF and INH, the results were interpreted using the absolute concentration method, wherein the development of < 20 colonies indicated susceptibility, and > 20 colonies indicated resistance to the respective antibiotic [77].

5. Conclusions

In the broader context, a structure resembling NSAIDs, such as carprofen, and a hydrazone-like structure can function as crucial pharmacophores in formulating prospective therapeutics against *M. tuberculosis*. This approach aims to enhance treatment success rates, particularly concerning MDR infections that contribute to substantial global morbidity and mortality. Extensive research is required to elucidate the intricate mechanisms of action of these molecules, along with assessing their biocompatibility and bioavailability properties, before progressing them to more advanced testing stages.

Supplementary Materials: The following supporting information can be downloaded at the website of this paper posted on Preprints.org. Figure S1: The ^{1}H-NMR spectra of (*EZ*)-N'-(4-bromobenzylidene-(2*RS*)-2-(6-chloro-9*H*-carbazol-2-yl)propane hydrazide (**1a**). Figure S2: The ^{13}C-NMR spectra of (*EZ*)-N'-(4-bromobenzylidene-(2*RS*)-2-(6-chloro-9*H*-carbazol-2-yl)propane hydrazide (**1a**). Figure S3: The APCI+ MS spectrum of **1a** in DMSO+MeOH. Figure S4: The experimental (up) and calculated (down) APCI+ MS spectra of **1a.** Figure S5: The ^{1}H-NMR spectra of (*EZ*)-N'-(2,6-difluorobenzylidene-(2*RS*)-2-(6-chloro-9*H*-carbazol-2-yl)propane hydrazide (**1b**). Figure S6: The ^{13}C-NMR spectra of (*EZ*)-N'-(2,6-difluorobenzylidene-(2*RS*)-2-(6-chloro-9*H*-carbazol-2-yl)propane hydrazide (**1b**). Figure S7: The APCI+ MS spectrum of **1b** in DMSO+MeOH. Figure S8: The experimental (up) and calculated (down) APCI+ MS spectra of **1b.** Figure S9: The ^{1}H-NMR spectra of (*EZ*)-N'-(3,4-difluorobenzylidene-(2*RS*)-2-(6-chloro-9*H*-carbazol-2-yl)propane hydrazide (**1c**). Figure S10: The ^{13}C-NMR spectra of (*EZ*)-N'-(3,4-difluorobenzylidene-(2*RS*)-2-(6-chloro-9*H*-carbazol-2-yl)propane hydrazide (**1c**). Figure S11: The APCI+ MS spectrum of **1c** in DMSO+MeOH. Figure S12: The experimental (up) and calculated (down) APCI+ MS spectra of **1c.** Figure S13: The ^{1}H-NMR spectra of (*EZ*)-N'-(2,3-dihydroxybenzylidene-(2*RS*)-2-(6-chloro-9*H*-carbazol-2-yl) propane hydrazide (**1d**). Figure S14: The ^{13}C-NMR spectra of (*EZ*)-N'-(2,3-dihydroxybenzylidene-(2*RS*)-2-(6-chloro-9*H*-carbazol-2-yl) propane hydrazide (**1d**). Figure S15: The APCI+ MS spectrum of **1d** in DMSO+MeOH. Figure S16: The experimental (up) and calculated (down) APCI+ MS spectra of **1d.** Figure S17: The ^{1}H-NMR spectra of (*EZ*)-N'-(2,4-dihydroxybenzylidene-(2*RS*)-2-(6-chloro-9*H*-carbazol-2-yl)propanehydrazide (**1e**). Figure S18: The ^{13}C-NMR spectra of (*EZ*)-N'-(2,4-dihydroxybenzylidene-(2*RS*)-2-(6-chloro-9*H*-carbazol-2-yl)propanehydrazide (**1e**). Figure S19: The APCI+ MS spectrum of **1e** in DMSO+MeOH. Figure S20: The experimental (up) and calculated (down) APCI+ MS spectra

of **1e.** Figure S21: The ^{1}H-NMR spectra of (*EZ*)-N'-(4-nitrobenzylidene-(2*RS*)-2-(6-chloro-9*H*-carbazol-2-yl)propane hydrazide (**1f**). Figure S22: The ^{13}C-NMR spectra of (*EZ*)-N'-(4-nitrobenzylidene-(2*RS*)-2-(6-chloro-9*H*-carbazol-2-yl)propane hydrazide (**1f**). Figure S23: The APCI+ MS spectrum of **1f** in DMSO+MeOH. Figure S24: The experimental (up) and calculated (down) APCI+ MS spectra of **1f.**

Author Contributions: Conceptualization, C.L. and I.M.V.; methodology, D.C.N., M.T.C., E.K., G.R.M. and S.A.; software, F.D., E.K. and V.A.C..; validation, M.T.C., F.D., E.K., S.A. and I.Z.; formal analysis, M.T.C., F.D., E.K.; investigation, D.C.N., G.R.M., A.G.N., I.Z., V.A.C. and A.M.B.; resources, I.M.V., G.R.M., V.A.C. and A.M.B.; data curation, C.L., G.R.M.; writing—original draft preparation, I.M.V. and C.L.; writing—review and editing, D.C.N.; visualization, I.Z.; supervision, D.C.N., G.R.M. and C.L.; project administration, D.C.N.; funding acquisition, I.M.V. All authors have read and agreed to the published version of the manuscript.

Funding: This research was funded by the EURO-MEDEX Project (33_PFE/2021)-29477/5.10.2022, Funder institution: Ministry of Research, Innovation, and Digitalization of Romania.

Data Availability Statement: We encourage all authors of articles published in MDPI journals to share their research data. In this section, please provide details regarding where data supporting reported results can be found, including links to publicly archived datasets analyzed or generated during the study. Where no new data were created, or where data is unavailable due to privacy or ethical restrictions, a statement is still required. Suggested Data Availability Statements are available in section "MDPI Research Data Policies" at https://www.mdpi.com/ethics.

Conflicts of Interest:The authors declare no conflicts of interest.

References

1. Palla, G.; Predieri, G.; Domiano, P.; Vignali, C.; Turner, W. Conformational behaviour and E/Z isomerization of N-acyl and N-aroylhydrazones. Tetrahedron 1986, 42, 3649-3654, doi:https://doi.org/10.1016/S0040-4020(01)87332-4.
2. Munir, R.; Javid, N.; Zia-ur-Rehman, M.; Zaheer, M.; Huma, R.; Roohi, A.; Athar, M.M. Synthesis of novel N-acylhydrazones and their CN/NN bond conformational characterization by NMR spectroscopy. Molecules 2021, 26, 4908.
3. Kümmerle, A.E.; Schmitt, M.; Cardozo, S.V.S.; Lugnier, C.; Villa, P.; Lopes, A.B.; Romeiro, N.C.; Justiniano, H.; Martins, M.A.; Fraga, C.A.M.; et al. Design, Synthesis, and Pharmacological Evaluation of N-Acylhydrazones and Novel Conformationally Constrained Compounds as Selective and Potent Orally Active Phosphodiesterase-4 Inhibitors. Journal of Medicinal Chemistry 2012, 55, 7525-7545, doi:10.1021/jm300514y.
4. Abdel-Rahman, H.M.; Abdel-Aziz, M.; Tinsley, H.N.; Gary, B.D.; Canzoneri, J.C.; Piazza, G.A. Design and Synthesis of Substituted Pyridazinone-1-Acetylhydrazones as Novel Phosphodiesterase 4 Inhibitors. Archiv der Pharmazie 2016, 349, 104-111, doi:10.1002/ardp.201500363.
5. Freitas, R.; Cordeiro, N.M.; Carvalho, P.R.; Alves, M.A.; Guedes, I.A.; Valerio, T.S.; Dardenne, L.E.; Lima, L.M.; Barreiro, E.J.; Fernandes, P.D.; et al. Discovery of naphthyl-N-acylhydrazone p38α MAPK inhibitors with *in vivo* anti-inflammatory and anti-TNF-α activity. Chemical biology & drug design 2018, 91, 391-397, doi:10.1111/cbdd.13085.
6. do Amaral, D.N.; Cavalcanti, B.C.; Bezerra, D.P.; Ferreira, P.M.P.; Castro, R.d.P.; Sabino, J.R.; Machado, C.M.L.; Chammas, R.; Pessoa, C.; Sant'Anna, C.M.R. Docking, synthesis and antiproliferative activity of N-acylhydrazone derivatives designed as combretastatin A4 analogues. PLoS One 2014, 9, e85380.
7. Fraga, C.A.; Barreiro, E.J. Medicinal chemistry of N-acylhydrazones: new lead-compounds of analgesic, antiinflammatory and antithrombotic drugs. Current medicinal chemistry 2006, 13, 167-198, doi:10.2174/092986706775197881.
8. Shin, S.Y.; Lee, J.; Ahn, S.; Yoo, M.; Lee, Y.H.; Koh, D.; Lim, Y. Design, synthesis, and evaluation of 4-chromenone derivatives combined with N-acylhydrazone for aurora kinase A inhibitor. Applied Biological Chemistry 2021, 64, 21, doi:10.1186/s13765-021-00596-4.
9. He, L.; Zhang, L.; Liu, X.; Li, X.; Zheng, M.; Li, H.; Yu, K.; Chen, K.; Shen, X.; Jiang, H.; et al. Discovering potent inhibitors against the beta-hydroxyacyl-acyl carrier protein dehydratase (FabZ) of Helicobacter pylori: structure-based design, synthesis, bioassay, and crystal structure determination. J Med Chem 2009, 52, 2465-2481, doi:10.1021/jm8015602.
10. Gorantla, V.; Gundla, R.; Jadav, S.S.; Anugu, S.R.; Chimakurthy, J.; Nidasanametla, S.K.; Korupolu, R. Molecular hybrid design, synthesis and biological evaluation of N-phenyl sulfonamide linked N-acyl hydrazone derivatives functioning as COX-2 inhibitors: new anti-inflammatory, anti-oxidant and anti-bacterial agents. New Journal of Chemistry 2017, 41, 13516-13532.
11. Zhang, H.; Kunadia, A.; Lin, Y.; Fondell, J.D.; Seidel, D.; Fan, H. Identification of a strong and specific antichlamydial N-acylhydrazone. PLOS ONE 2017, 12, e0185783, doi:10.1371/journal.pone.0185783.

12. Gu, W.; Wu, R.; Qi, S.; Gu, C.; Si, F.; Chen, Z. Synthesis and Antibacterial Evaluation of New N-acylhydrazone Derivatives from Dehydroabietic Acid. Molecules 2012, 17, 4634-4650, doi:10.3390/molecules17044634.
13. Dos Santos Fernandes, G.F.; de Souza, P.C.; Moreno-Viguri, E.; Santivañez-Veliz, M.; Paucar, R.; Pérez-Silanes, S.; Chegaev, K.; Guglielmo, S.; Lazzarato, L.; Fruttero, R.; et al. Design, Synthesis, and Characterization of N-Oxide-Containing Heterocycles with *in Vivo* Sterilizing Antitubercular Activity. J Med Chem 2017, 60, 8647-8660, doi:10.1021/acs.jmedchem.7b01332.
14. Cardoso, S.H.; Barreto, M.B.; Lourenço, M.C.; Henriques, M.; Candéa, A.L.; Kaiser, C.R.; de Souza, M.V. Antitubercular activity of new coumarins. Chemical biology & drug design 2011, 77, 489-493, doi:10.1111/j.1747-0285.2011.01120.x.
15. Rozada, A.M.; Rodrigues, F.A.; Sampiron, E.G.; Seixas, F.A.; Basso, E.A.; Scodro, R.B.; Kioshima É, S.; Gauze, G.F. Novel 4-methoxynaphthalene-N-acylhydrazones as potential for paracoccidioidomycosis and tuberculosis co-infection. Future microbiology 2019, 14, 587-598, doi:10.2217/fmb-2018-0357.
16. Dos Santos Filho, J.M.; de Queiroz, E.S.D.M.A.; Macedo, T.S.; Teixeira, H.M.P.; Moreira, D.R.M.; Challal, S.; Wolfender, J.L.; Queiroz, E.F.; Soares, M.B.P. Conjugation of N-acylhydrazone and 1,2,4-oxadiazole leads to the identification of active antimalarial agents. Bioorganic & medicinal chemistry 2016, 24, 5693-5701, doi:10.1016/j.bmc.2016.09.013.
17. Carvalho, S.A.; Kaiser, M.; Brun, R.; Silva, E.F.; Fraga, C.A. Antiprotozoal Activity of (E)-Cinnamic N-Acylhydrazone Derivatives. Molecules 2014, 19, 20374-20381, doi:10.3390/molecules191220374.
18. Alves, M.S.D.; das Neves, R.N.; Sena-Lopes, Â.; Domingues, M.; Casaril, A.M.; Segatto, N.V.; Nogueira, T.C.M.; de Souza, M.V.N.; Savegnago, L.; Seixas, F.K.; et al. Antiparasitic activity of furanyl N-acylhydrazone derivatives against Trichomonas vaginalis: *in vitro* and in silico analyses. Parasites & Vectors 2020, 13, 59, doi:10.1186/s13071-020-3923-8.
19. Kumar, P.; Kadyan, K.; Duhan, M.; Sindhu, J.; Singh, V.; Saharan, B.S. Design, synthesis, conformational and molecular docking study of some novel acyl hydrazone based molecular hybrids as antimalarial and antimicrobial agents. Chemistry Central Journal 2017, 11, 115, doi:10.1186/s13065-017-0344-7.
20. Silva, D.K.C.; Teixeira, J.S.; Moreira, D.R.M.; da Silva, T.F.; Barreiro, E.J.L.; de Freitas, H.F.; Pita, S.; Teles, A.L.B.; Guimarães, E.T.; Soares, M.B.P. *In Vitro*, *In Vivo* and In Silico Effectiveness of LASSBio-1386, an N-Acyl Hydrazone Derivative Phosphodiesterase-4 Inhibitor, Against Leishmania amazonensis. Frontiers in pharmacology 2020, 11, 590544, doi:10.3389/fphar.2020.590544.
21. Xiao, M.; Ye, J.; Lian, W.; Zhang, M.; Li, B.; Liu, A.; Hu, A. Microwave-assisted synthesis, characterization and bioassay of acylhydrazone derivatives as influenza neuraminidase inhibitors. Medicinal Chemistry Research 2017, 26, 3216-3227.
22. Rodrigues, D.A.; Ferreira-Silva, G.; Ferreira, A.C.; Fernandes, R.A.; Kwee, J.K.; Sant'Anna, C.M.; Ionta, M.; Fraga, C.A. Design, Synthesis, and Pharmacological Evaluation of Novel N-Acylhydrazone Derivatives as Potent Histone Deacetylase 6/8 Dual Inhibitors. J Med Chem 2016, 59, 655-670, doi:10.1021/acs.jmedchem.5b01525.
23. Cordeiro, N.M.; Freitas, R.H.; Fraga, C.A.; Fernandes, P.D. Discovery of Novel Orally Active Tetrahydro-Naphthyl-N-Acylhydrazones with *In Vivo* Anti-TNF-α Effect and Remarkable Anti-Inflammatory Properties. PLoS One 2016, 11, e0156271, doi:10.1371/journal.pone.0156271.
24. Polo-Cerón, D.; Hincapié-Otero, M.M.; Joaqui-Joaqui, A. Synthesis and characterization of four N-acylhydrazones as potential O, N, O donors for Cu2+: An experimental and theoretical study. Universitas Scientiarum 2021, 26, 193-215.
25. Thiago Moreira, P.; Arthur Eugen, K. Hydrazone-Based Small-Molecule Chemosensors. In Computational Biology and Chemistry, Payam, B., Nicola, B., Eds.; IntechOpen: Rijeka, 2020; p. Ch. 6.
26. Guay, D.R. An update on the role of nitrofurans in the management of urinary tract infections. Drugs 2001, 61, 353-364, doi:10.2165/00003495-200161030-00004.
27. McOsker, C.C.; Fitzpatrick, P.M. Nitrofurantoin: mechanism of action and implications for resistance development in common uropathogens. The Journal of antimicrobial chemotherapy 1994, 33 Suppl A, 23-30, doi:10.1093/jac/33.suppl_a.23.
28. Basile, M.; Gidaro, S.; Pacella, M.; Biffignandi, P.M.; Gidaro, G.S. Troxerutin-carbazochrome combination versus placebo in the treatment of posthemorrhoidectomy symptoms: a single-center, randomized, double-blind, placebo-controlled study. Current Therapeutic Research 2002, 63, 527-535, doi:https://doi.org/10.1016/S0011-393X(02)80058-3.
29. Passali, G.C.; De Corso, E.; Bastanza, G.; Di Gennaro, L. An old drug for a new application: carbazochrome-sodium-sulfonate in HHT. Journal of clinical pharmacology 2015, 55, 601-602, doi:10.1002/jcph.452.
30. Krause, T.; Gerbershagen, M.U.; Fiege, M.; Weisshorn, R.; Wappler, F. Dantrolene--a review of its pharmacology, therapeutic use and new developments. Anaesthesia 2004, 59, 364-373, doi:10.1111/j.1365-2044.2004.03658.x.

31. Corrêa, J.C.R.; Hiene, M.A.C.; Salgado, H.R.N. Physico-chemical characterization and analytical development for sodium azumolene, a potential drug designed to fight malignant hyperthermia. Journal of Analytical & Bioanalytical Techniques 2013, 1-6.
32. Sachdev, E.; Sachdev, D.; Mita, M. Aldoxorubicin for the treatment of soft tissue sarcoma. Expert opinion on investigational drugs 2017, 26, 1175-1179, doi:10.1080/13543784.2017.1371134.
33. Costa, D.G.; da Silva, J.S.; Kümmerle, A.E.; Sudo, R.T.; Landgraf, S.S.; Caruso-Neves, C.; Fraga, C.A.; de Lacerda Barreiro, E.J.; Zapata-Sudo, G. LASSBio-294, A compound with inotropic and lusitropic activity, decreases cardiac remodeling and improves $Ca^{2}(+)$ influx into sarcoplasmic reticulum after myocardial infarction. American journal of hypertension 2010, 23, 1220-1227, doi:10.1038/ajh.2010.157.
34. Silva, C.L.; Noël, F.; Barreiro, E.J. Cyclic GMP-dependent vasodilatory properties of LASSBio 294 in rat aorta. British journal of pharmacology 2002, 135, 293-298, doi:10.1038/sj.bjp.0704473.
35. Lucas, P.W.; Schmit, J.M.; Peterson, Q.P.; West, D.C.; Hsu, D.C.; Novotny, C.J.; Dirikolu, L.; Churchwell, M.I.; Doerge, D.R.; Garrett, L.D.; et al. Pharmacokinetics and derivation of an anticancer dosing regimen for PAC-1, a preferential small molecule activator of procaspase-3, in healthy dogs. Investigational new drugs 2011, 29, 901-911, doi:10.1007/s10637-010-9445-z.
36. Peterson, Q.P.; Goode, D.R.; West, D.C.; Ramsey, K.N.; Lee, J.J.; Hergenrother, P.J. PAC-1 activates procaspase-3 *in vitro* through relief of zinc-mediated inhibition. Journal of molecular biology 2009, 388, 144-158, doi:10.1016/j.jmb.2009.03.003.
37. Thota, S.; Rodrigues, D.A.; Pinheiro, P.d.S.M.; Lima, L.M.; Fraga, C.A.M.; Barreiro, E.J. N-Acylhydrazones as drugs. Bioorganic & Medicinal Chemistry Letters 2018, 28, 2797-2806, doi:https://doi.org/10.1016/j.bmcl.2018.07.015.
38. Effenberger, K.; Breyer, S.; Ocker, M.; Schobert, R. New doxorubicin N-acyl hydrazones with improved efficacy and cell line specificity show modes of action different from the parent drug. International journal of clinical pharmacology and therapeutics 2010, 48, 485-486, doi:10.5414/cpp48485.
39. de Melo, T.R.; Chelucci, R.C.; Pires, M.E.; Dutra, L.A.; Barbieri, K.P.; Bosquesi, P.L.; Trossini, G.H.; Chung, M.C.; dos Santos, J.L. Pharmacological evaluation and preparation of nonsteroidal anti-inflammatory drugs containing an N-acyl hydrazone subunit. International journal of molecular sciences 2014, 15, 5821-5837, doi:10.3390/ijms15045821.
40. Aarjane, M.; Aouidate, A.; Slassi, S.; Amine, A. Synthesis, antibacterial evaluation, in silico ADMET and molecular docking studies of new N-acylhydrazone derivatives from acridone. Arabian Journal of Chemistry 2020, 13, 6236-6245, doi:https://doi.org/10.1016/j.arabjc.2020.05.034.
41. Lazzarini, C.; Haranahalli, K.; Rieger, R.; Ananthula Hari, K.; Desai Pankaj, B.; Ashbaugh, A.; Linke Michael, J.; Cushion Melanie, T.; Ruzsicska, B.; Haley, J.; et al. Acylhydrazones as Antifungal Agents Targeting the Synthesis of Fungal Sphingolipids. Antimicrobial Agents and Chemotherapy 2018, 62, 10.1128/aac.00156-00118, doi:10.1128/aac.00156-18.
42. Nogueira, T.C.M.; dos Santos Cruz, L.; Lourenço, M.C.; de Souza, M.V.N. Design, synthesis and anti-tuberculosis activity of hydrazones and N-acylhydrazones containing vitamin B6 and different heteroaromatic nucleus. Letters in Drug Design & Discovery 2019, 16, 792-798.
43. Angelova, V.T.; Valcheva, V.; Vassilev, N.G.; Buyukliev, R.; Momekov, G.; Dimitrov, I.; Saso, L.; Djukic, M.; Shivachev, B. Antimycobacterial activity of novel hydrazide-hydrazone derivatives with 2H-chromene and coumarin scaffold. Bioorganic & Medicinal Chemistry Letters 2017, 27, 223-227, doi:https://doi.org/10.1016/j.bmcl.2016.11.071.
44. Fernandes, G.F.d.S.; de Souza, P.C.; Marino, L.B.; Chegaev, K.; Guglielmo, S.; Lazzarato, L.; Fruttero, R.; Chung, M.C.; Pavan, F.R.; dos Santos, J.L. Synthesis and biological activity of furoxan derivatives against Mycobacterium tuberculosis. European Journal of Medicinal Chemistry 2016, 123, 523-531, doi:https://doi.org/10.1016/j.ejmech.2016.07.039.
45. Naveen Kumar, H.S.; Parumasivam, T.; Jumaat, F.; Ibrahim, P.; Asmawi, M.Z.; Sadikun, A. Synthesis and evaluation of isonicotinoyl hydrazone derivatives as antimycobacterial and anticancer agents. Medicinal Chemistry Research 2014, 23, 269-279.
46. Fahmi, M.R.G.; Khumaidah, L.; Ilmiah, T.K.; Fadlan, A.; Santoso, M. 2-Thiophenecarboxylic acid hydrazide Derivatives: Synthesis and Anti-Tuberculosis Studies. IOP Conference Series: Materials Science and Engineering 2018, 349, 012039, doi:10.1088/1757-899X/349/1/012039.
47. Joshi, S.D.; Dixit, S.R.; Gadag, S.; Kulkarni, V.H.; Aminabhavi, T.M. Molecular docking, synthesis, and antimycobacterial activities of pyrrolyl hydrazones and their copper complexes. Research and Reports in Medicinal Chemistry 2015, 1-14.
48. Bordei, A.T.; Nuță, D.C.; Musat, G.C.; Missir, A.V.; Caproiu, M.T.; Dumitrascu, F.; Zarafu, I.; Ionita, P.; Badiceanu, C.D.; Limban,C.L. Microwave assisted synthesis and spectroscopic characterization of some novel Schiff bases of carprofen hydrazide. Farmacia 2019, 67, 955-962.
49. Avram, S.; Udrea, A.M.; Nuta, D.C.; Limban, C.; Balea, A.C.; Caproiu, M.T.; Dumitrascu, F.; Buiu, C.; Bordei, A.T. Synthesis and Bioinformatic Characterization of New Schiff Bases with Possible Applicability in Brain Disorders. Molecules 2021, 26, doi:10.3390/molecules26144160.

50. Bordei, A.T.; Limban, C.; Nuta, D.C.; Zarafu, I.; Denes, M.; Marutescu, L.; Chifiriuc, M.C.; Popa, M.; Arama, C. Recent advances in the study of derivatives of (EZ)-N'-benzylidene-(2RS)-2-(6-chloro-9h-carbazol-2-yl)propanohydrazide. Farmacia 2022, 70, 589-595.
51. Singh, V.; Chibale, K. Strategies to Combat Multi-Drug Resistance in Tuberculosis. Accounts of Chemical Research 2021, 54, 2361-2376, doi:10.1021/acs.accounts.0c00878.
52. Nguyen, L. Antibiotic resistance mechanisms in M. tuberculosis: an update. Archives of toxicology 2016, 90, 1585-1604, doi:10.1007/s00204-016-1727-6.
53. Bendre, A.D.; Peters, P.J.; Kumar, J. Tuberculosis: Past, present and future of the treatment and drug discovery research. Current research in pharmacology and drug discovery 2021, 2, 100037.
54. Riccardi, G.; Pasca, M.R.; Buroni, S. Mycobacterium tuberculosis: drug resistance and future perspectives. Future microbiology 2009, 4, 597-614, doi:10.2217/fmb.09.20.
55. Sarkar, D.; Maiti, A.K.; Alenazy, R.; Joseph, B. In silico Approach to Identify Potent Bioactive Compounds as Inhibitors against the Enoyl-acyl Carrier Protein (acp) Reductase Enzyme of Mycobacterium tuberculosis. 2021.
56. Iacobino, A.; Fattorini, L.; Giannoni, F. Drug-Resistant Tuberculosis 2020: Where We Stand. Applied Sciences 2020, 10, doi:10.3390/app10062153.
57. Zhang, Y.; Yew, W.W. Mechanisms of drug resistance in Mycobacterium tuberculosis: update 2015. The international journal of tuberculosis and lung disease : the official journal of the International Union against Tuberculosis and Lung Disease 2015, 19, 1276-1289, doi:10.5588/ijtld.15.0389.
58. Singh, R.; Dwivedi, S.P.; Gaharwar, U.S.; Meena, R.; Rajamani, P.; Prasad, T. Recent updates on drug resistance in Mycobacterium tuberculosis. Journal of applied microbiology 2020, 128, 1547-1567, doi:10.1111/jam.14478.
59. Ozma, M.A.; Lahouty, M.; Abbasi, A.; Rezaee, M.A.; Kafil, H.S.; Asgharzadeh, M. Effective bacterial factors involved in the dissemination of tuberculosis. 2022.
60. Dhameliya, T.M.; Vekariya, D.D.; Patel, H.Y.; Patel, J.T. Comprehensive coverage on anti-mycobacterial endeavour reported during 2022. European Journal of Medicinal Chemistry 2023, 255, 115409, doi:https://doi.org/10.1016/j.ejmech.2023.115409.
61. Palomino, J.C.; Martin, A. Drug resistance mechanisms in Mycobacterium tuberculosis. Antibiotics 2014, 3, 317-340.
62. Khawbung, J.L.; Nath, D.; Chakraborty, S. Drug resistant Tuberculosis: A review. Comparative immunology, microbiology and infectious diseases 2021, 74, 101574, doi:10.1016/j.cimid.2020.101574.
63. Mabhula, A.; Singh, V. Drug-resistance in Mycobacterium tuberculosis: where we stand. MedChemComm 2019, 10, 1342-1360, doi:10.1039/c9md00057g.
64. Khan, Z.; Ualiyeva, D.; Jamal, K.; Ali, B.; Ahmad, F.; Sapkota, S.; Boadi Amissah, O.; Ndip Ndip Bate, P. Molecular diagnostics and potential therapeutic options for mycobacterium tuberculosis: Where we stand. Medicine in Omics 2023, 8, 100022, doi:https://doi.org/10.1016/j.meomic.2023.100022.
65. Mirnejad, R.; Asadi, A.; Khoshnood, S.; Mirzaei, H.; Heidary, M.; Fattorini, L.; Ghodousi, A.; Darban-Sarokhalil, D. Clofazimine: A useful antibiotic for drug-resistant tuberculosis. Biomedicine & pharmacotherapy = Biomedecine & pharmacotherapie 2018, 105, 1353-1359, doi:10.1016/j.biopha.2018.06.023.
66. Raghu, M.S.; Kumar, C.B.P.; Kumar, K.Y.; Prashanth, M.K.; Alshahrani, M.Y.; Ahmad, I.; Jain, R. Design, synthesis and molecular docking studies of imidazole and benzimidazole linked ethionamide derivatives as inhibitors of InhA and antituberculosis agents. Bioorganic & Medicinal Chemistry Letters 2022, 60, 128604.
67. Veena, K.; Raghu, M.S.; Kumar, K.Y.; Kumar, C.B.P.; Alharti, F.A.; Prashanth, M.K.; Jeon, B.-H. Design and synthesis of novel benzimidazole linked thiazole derivatives as promising inhibitors of drug-resistant tuberculosis. Journal of Molecular Structure 2022, 1269, 133822.
68. Acharya, P.T.; Bhavsar, Z.A.; Jethava, D.J.; Rajani, D.P.; Pithawala, E.; Patel, H.D. Synthesis, characterization, biological evaluation, and computational study of benzimidazole hybrid thiosemicarbazide derivatives. Journal of Heterocyclic Chemistry 2022, 59, 2142-2164.
69. Sahoo, S.K.; Maddipatla, S.; Gajula, S.N.R.; Ahmad, M.N.; Kaul, G.; Nanduri, S.; Sonti, R.; Dasgupta, A.; Chopra, S.; Yaddanapudi, V.M. Identification of nitrofuranylchalcone tethered benzoxazole-2-amines as potent inhibitors of drug resistant Mycobacterium tuberculosis demonstrating bactericidal efficacy. Bioorganic & Medicinal Chemistry 2022, 64, 116777.
70. Vassiliades, S.V.; Navarausckas, V.B.; Dias, M.V.B.; Parise Filho, R. Mycobacterium tuberculosis dihydrofolate reductase inhibitors: State of Art Past 20 Years. Biointerface Research in Applied Chemistry 2023, 13.
71. Pradhan, M.; Nanda, B.; Kar, P.; Nanda, B.B. Intermolecular interactions of anti-tuberculosis drugs with different solvents: a review. Biointerface Research in Applied Chemistry 2022, 12, 883-892.
72. Hernández-Viveros, D.; Rechy-Iruretagoyena, D.A.; Díaz-Molina, R.; Vique-Sánchez, J.L. Triosephosphate Isomerase from Mycobacterium tuberculosis as Potential Target to Develop a New Anti-TB Drug. 2021.

73. Kancharla, S.K.; Birudaraju, S.; Pal, A.; Reddy, L.K.; Reddy, E.R.; Vagolu, S.K.; Sriram, D.; Bonige, K.B.; Korupolu, R.B. Synthesis and biological evaluation of isatin oxime ether-tethered aryl 1 H-1, 2, 3-triazoles as inhibitors of Mycobacterium tuberculosis. New Journal of Chemistry 2022, 46, 2863-2874.
74. Chitti, S.; Van Calster, K.; Cappoen, D.; Nandikolla, A.; Khetmalis, Y.M.; Cos, P.; Kumar, B.K.; Murugesan, S.; Sekhar, K.V.G.C. Design, synthesis and biological evaluation of benzo-[d]-imidazo-[2, 1-b]-thiazole and imidazo-[2, 1-b]-thiazole carboxamide triazole derivatives as antimycobacterial agents. RSC advances 2022, 12, 22385-22401.
75. Shinde, S.R.; Inamdar, S.N.; Shinde, M.; Pawar, C.; Kushwaha, B.; Obakachi, V.A.; Kajee, A.; Chauhan, R.; Karpoormath, R. Discovery of oxazoline-triazole based hybrid molecules as DNA gyrase inhibitors: A new class of potential Anti-tubercular agents. Journal of Molecular Structure 2023, 1273, 134243.
76. El-Shoukrofy, M.S.; Atta, A.; Fahmy, S.; Sriram, D.; Mahran, M.A.; Labouta, I.M. New tetrahydropyrimidine-1, 2, 3-triazole clubbed compounds: Antitubercular activity and Thymidine Monophosphate Kinase (TMPKmt) inhibition. Bioorganic Chemistry 2023, 131, 106312.
77. Homorodean, D.; Moisoiu, A.; Borroni, E. Ghid național pentru rețeaua laboratoarelor TB, Ministerul Sănătății 2017.